Hydrogenic and screened self-energies for *d* states

J. Sapirstein*

Department of Physics, University of Notre Dame, Notre Dame, Indiana 46556, USA

K. T. Cheng†

University of California, Lawrence Livermore National Laboratory, Livermore, California 94550, USA

The one-loop self-energy is evaluated for $d_{3/2}$ and $d_{5/2}$ states in hydrogenic ions, and good agreement found with previous calculations. Results are compared to what is known of the $Z\alpha$ expansion and higher-order binding corrections inferred for these states as well as for their fine structures. Screened Kohn-Sham potentials are then used to evaluate the one-loop self-energy corrections to $n=2$ states of lithiumlike ions for $Z = 10$–100, $n=3$ states of sodiumlike ions for $Z=20$–100, and $n=4$ states of copperlike ions for $Z=40$–100. The importance of these screened calculations for the interpretation of recent high accuracy experiments is emphasized.

PACS number(s): 31.30.Jv, 12.20.Ds

I. INTRODUCTION

The one-loop self-energy has been extensively studied both as an expansion in $Z\alpha$ and $\ln(Z\alpha)$ and in an exact manner using various numerical techniques: a useful review of the theory has been given by Mohr in Ref. [1]. The numerical approach, starting with the basic idea of Brown, Langer, and Schaefer [2] in the late 1950s, was first correctly implemented in the calculations of Desiderio and Johnson [3] in the early 1970s. A different, and more accurate, numerical approach was developed by Mohr [4] for hydrogenic ions at around the same time. Exploiting the analytic control available when the Dirac-Coulomb Green's function is expressed in terms of Whittaker functions, Mohr and collaborators have systematically increased the accuracy of their method, which applies primarily to one-electron atoms with a point nucleus [5,6], but has been extended to the case of a finite nucleus modeled as either a shell or uniform distribution of charge [7]. The method of Brown *et al.* [2], however, can be applied to any local central potential, and a number of groups have developed methods to calculate self-energies in potentials more appropriate to many-electron atoms, with greater accuracy afforded by further subtractions of the electron propagator [8], as will be described in more detail below. In this paper, we will describe extensions of a method that we have developed in collaboration with Johnson [9]. Other groups have also treated the problem of self-energies in many-electron systems. We note in particular calculations carried out around the same time as our earlier work by Blundell and Snyderman [10] and the Göteborg group [11], and more recent computational methods developed by Shabaev and Yerokhin [12] and Goidenko *et al.* [13].

It is the purpose of this paper to first briefly describe the method of Ref. [9], which has significantly been improved in accuracy since its first introduction. We then apply the method to calculations of the self-energy for point-Coulomb hydrogenic ions in the $nd_{3/2}$ and $nd_{5/2}$ states with $n=3$ and 4, with the purpose of comparing with earlier work and making a comparison with the $Z\alpha$ expansion, particularly for the fine structure of these states. Since experiments on highly charged, many-electron ions are producing more and more high-precision spectroscopic data, we also present tables of self-energy contributions in realistic local potentials for $n=2$ lithiumlike, $n=3$ sodiumlike, and $n=4$ copperlike ions, including ns and np states in addition to nd states for completeness.

In the next section, improvements in our method for calculating the one-loop self-energy are described. In the following section, 3d and 4d results for hydrogenic systems are presented and compared with those from the $Z\alpha$ expansion. Screened results using Kohn-Sham model potentials are presented in the next section, and the role of the present calculation for the interpretation of a recent high-accuracy experiment in copperlike ions [14] is discussed in the conclusion.

II. CALCULATIONAL SCHEME

Because the method used to evaluate the self-energy has been given in some detail in Ref. [9], we describe it here only schematically. The basic idea is to rewrite the electron propagator in an arbitrary local central potential $V(r)$ as

$$S_F = (S_F - S_0 - S_0 V S_0) + (S_0 + S_0 V S_0) \equiv S_F^{\text{main}} + S_F^{\text{pspace}},$$
(1)

where S_0 is the free electron propagator. Specifically

$$S_F^{\text{main}}(\vec{x},\vec{y};E) = S_F(\vec{x},\vec{y};E) - S_0(\vec{x},\vec{y};E)$$
$$- \int d^3 r S_0(\vec{x},\vec{r};E) V(r) S_0(\vec{r},\vec{y};E)$$
(2)

and

*Electronic address: jsapirst@nd.edu
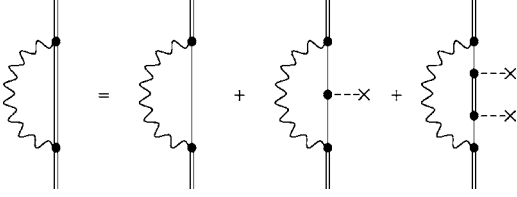†Electronic address: ktcheng@llnl.gov

FIG. 1. The expansion of the electron self-energy into zero-, one-, and two-potential terms. Single and double lines refer to free and bound electrons, respectively. Dashed lines ending with a cross refer to interactions with the potential $V(r)$.

$$S_F^{\text{pspace}} = S_0(\vec{x},\vec{y};E) + \int d^3r S_0(\vec{x},\vec{r};E)V(r)S_0(\vec{r},\vec{y};E). \quad (3)$$

When the electron propagator in the dimensionally regularized self-energy of state v,

$$\Sigma_{vv} = -ie^2 \int d^3x \int d^3y \int \frac{d^nk}{(2\pi)^n} \frac{e^{ik\cdot(\vec{x}-\vec{y})}}{k^2+i\delta} \bar{\psi}_v(\vec{x})\gamma_\mu$$
$$\times S_F(\vec{x},\vec{y};\epsilon_v-k_0)\gamma^\mu\psi_v(\vec{y}), \quad (4)$$

is replaced with S_F^{main}, an ultraviolet finite expression is encountered that can be evaluated in coordinate space after partial wave expansions of the propagators are made. Mathematically, this is equivalent to the direct evaluation of the ultraviolet finite "two-potential" term $\Sigma_{vv}(S_0VS_FVS_0)$, the last term in the expansion of the electron self-energy in an external potential V shown in Fig. 1, an approach proposed by Snyderman [8].

The bound and free propagators can be formed from combinations of solutions of the Dirac equation regular at either the origin or infinity [15]. Here, radial functions of these solutions are obtained numerically, partial wave by partial wave, using an Adams predictor-corrector method modified to handle high angular momentum states l and high photon energies $\omega=k_0$. This numerical approach works for any local potential, including $V(r)=-Z\alpha/r$ for point-Coulomb potentials and, in particular, $V(r)=0$ so that the free propagator S_0 is evaluated in exactly the same way as the bound propagator S_F, greatly simplifying the numerical calculations. While significant cancellation takes place between the three components of S_F^{main}, present computer capability allows the use of extremely fine radial grids with 5000–50 000 points, which leads to control of the calculation to high partial waves, typically up to $l=50$ without any problem. An advantage of being able to calculate high-l terms directly is the fact that in some cases the $1/l^3$ asymptotic behavior of the partial wave series is not reached at lower values. This happens when the partial wave series converges very slowly, as is usually the case for low-Z ions or for the valence states of near neutral atoms, or when a sign change of the series occurs at intermediate-l values. Once the series is close to its asymptotic limit, contributions from higher-l partial waves can be obtained by extrapolation with accelerated convergence methods to achieve higher accuracy. While under good control in general, the high-l behavior is still the ultimate limit of the accuracy of this method. However, this problem is greatly ameliorated when fine structure is considered, as the difficult high-l terms cancel substantially. We will exploit this fact when treating hydrogenic d states, where we will be able to provide answers for the fine structure an order of magnitude more accurate than for the individual states. We note that high-l partial waves of bound states with the same principal quantum number n also largely cancel, making self-energy corrections to intrashell ($\Delta n=0$) transitions significantly easier to calculate than self-energies of individual states, an effect noted in Ref. [16].

When the Wick rotation $k_0 \to i\omega$ is carried out, poles are passed that are easily evaluated. However, the small-ω region of the integral can suffer from numerical instabilities associated with the fact that the energy of the bound electron propagator $E=\epsilon_v-i\omega$ is very close to the eigenenergy of the bound state ϵ_v. The source of the problem is that for the partial wave with angular quantum number $\kappa=\kappa_v$, the two independent solutions of the Dirac equation with $E=\epsilon_v-i\omega$ regular at the origin and at infinity, which are used to form the electron Green's function as mentioned earlier, are now both very close to the eigenfunction of the bound state v, resulting in severe numerical cancellation and rapid loss of accuracy as $\omega \to 0$. This problem can be eliminated by introducing a regulator δ through $\epsilon_v \to (1-\delta)\epsilon_v$ and taking the limit $\delta \to 0$ for the affected partial waves. In particular, the extrapolation to $\delta=0$ can be avoided altogether by taking the average of the results regulated with $|\delta|$ and $-|\delta|$. This symmetric-averaging approach is found to give very accurate results when changes in the pole term contributions due to the introduction of the regulators are properly taken into account.

The remaining part of the calculation involving S_F^{pspace} are individually ultraviolet divergent in the limit $n \to 4$, but these divergences can be analytically isolated, and completely cancel when the self-mass counter term is included. The ultraviolet finite terms remaining are evaluated in momentum space, with the "zero-potential" S_0 term being a two-dimensional integral and the "one-potential" S_0VS_0 term initially a five-dimensional integral that we reduce to four dimensions by carrying out one of the Feynman parameter integrals. The needed Fourier transforms of the bound-state wave function ψ_v are carried out using a modification of Filon's method which works for nonlinear radial grids commonly used in atomic structure calculations. The numerical four-dimensional integrations are carried out with very high accuracy with the use of the multidimensional integration routine CUHRE, a part of the CUBA suite of integration programs described in Ref. [17]. While not presented here, we note that accurate methods for the treatment of vacuum polarization are described in Ref. [18], and can easily be applied to d states.

III. POINT NUCLEUS HYDROGEN RESULTS

The one-loop self-energy is given in terms of the dimensionless function $F(Z\alpha)$ as

$$E_{\text{SE}} = \frac{\alpha}{\pi} \frac{(Z\alpha)^4}{n^3} F(Z\alpha)mc^2. \quad (5)$$

Results for $d_{3/2}$ states of hydrogenic ions with $Z=10–110$ have been reported in Ref. [5], while those for $d_{5/2}$ states

TABLE I. $F(Z\alpha)$ for the hydrogenic 3d and 4d states and their fine structure (f.s.) splittings.

Z	$3d_{3/2}$	$3d_{5/2}$	f.s. (3d)	$4d_{3/2}$	$4d_{5/2}$	f.s. (4d)
10	−0.0427	0.0407	0.0834	−0.0407	0.0428	0.0835
20	−0.0420	0.0417	0.0838	−0.0399	0.0439	0.0839
30	−0.0410	0.0432	0.0843	−0.0387	0.0457	0.0844
40	−0.0396	0.0452	0.0848	−0.0371	0.0479	0.0850
50	−0.0378	0.0475	0.0853	−0.0348	0.0507	0.0855
60	−0.0353	0.0503	0.0857	−0.0318	0.0541	0.0858
70	−0.0321	0.0536	0.0857	−0.0277	0.0580	0.0856
80	−0.0279	0.0572	0.0851	−0.0222	0.0624	0.0846
90	−0.0225	0.0612	0.0837	−0.0149	0.0673	0.0822
100	−0.0154	0.0654	0.0808	−0.0053	0.0727	0.0779

with $Z=60-110$ have been given in Ref. [19]. We find good agreement with these results, and present our 3d and 4d results with $Z=10-100$ in Table I. As mentioned above, difficulties in the precise extrapolation of the partial wave summation limit our accuracy for individual states. In general, we calculate up to $l=50$ which is good enough to give $F(Z\alpha)$ accurate to four digits past the decimal point in most cases. But for $Z=10$ in three dimensions and $Z=10$ and 20 in four dimensions, the convergence of the partial wave series is so slow that even with l going up to 70, it is still difficult to maintain the same level of accuracy. Specifically, for the 4d results at $Z=20$, uncertainties in $F(Z\alpha)$ are close to 1% at about 0.0004. For the 3d and 4d results at $Z=10$, however, uncertainties can be two to five times higher. For these low-Z ions, the results in Table I are derived from the known $Z\alpha$ expansion [20]

$$F(3d_{3/2}) = -\frac{1}{20} - \frac{4}{3}\ln k_0(3d) + \left[\frac{4}{405}\ln(Z\alpha)^{-2}\right.$$
$$\left. + 0.005551573(2)\right](Z\alpha)^2, \tag{6}$$

$$F(3d_{5/2}) = \frac{1}{30} - \frac{4}{3}\ln k_0(3d) + \left[\frac{4}{405}\ln(Z\alpha)^{-2}\right.$$
$$\left. + 0.027609989(2)\right](Z\alpha)^2, \tag{7}$$

$$F(4d_{3/2}) = -\frac{1}{20} - \frac{4}{3}\ln k_0(4d) + \left[\frac{1}{90}\ln(Z\alpha)^{-2}\right.$$
$$\left. + 0.005585985(2)\right](Z\alpha)^2, \tag{8}$$

$$F(4d_{5/2}) = \frac{1}{30} - \frac{4}{3}\ln k_0(4d) + \left[\frac{1}{90}\ln(Z\alpha)^{-2}\right.$$
$$\left. + 0.031411862(2)\right](Z\alpha)^2, \tag{9}$$

where the first ten significant digits of the Bethe logarithm terms are [21]

$$\ln k_0(3d) = -0.005\,232\,148\,141, \tag{10}$$

$$\ln k_0(4d) = -0.006\,740\,938\,877. \tag{11}$$

By fitting the difference between the calculated and the analytic results for $Z>30$ to higher-order $Z\alpha$-expansion terms, we can extend the above equations to include additional $(Z\alpha)^4$ terms with coefficients given by 0.12(1), 0.07(1), 0.16(1), and 0.09(1) for $F(3d_{3/2})$, $F(3d_{5/2})$, $F(4d_{3/2})$, and $F(4d_{5/2})$, respectively. In Figs. 2 and 3, calculated results are compared with the analytic ones with and without the fitted $(Z\alpha)^4$ terms for $F(3d_{3/2})$ and $F(3d_{5/2})$, respectively. It can be seen that analytic results from the above equations are good up to about $Z=20$ but deviate more and more from the calculated results beyond that point. The addition of the fitted $(Z\alpha)^4$ terms extends the validity of the $Z\alpha$ expansions to $Z=40$. Similar behaviors are found for $F(4d_{3/2})$ and $F(4d_{5/2})$ and are not shown here. By using analytic results with the fitted $(Z\alpha)^4$ terms for $Z=10$ and 20, results in Table I should be consistently accurate to the last digit shown.

While accuracies of our $d_{3/2}$ and $d_{5/2}$ results at low-Z are severely limited by the slow convergence of the partial wave series, those of the fine structures $d_{5/2}-d_{3/2}$ are under much better control because of strong cancellations between the
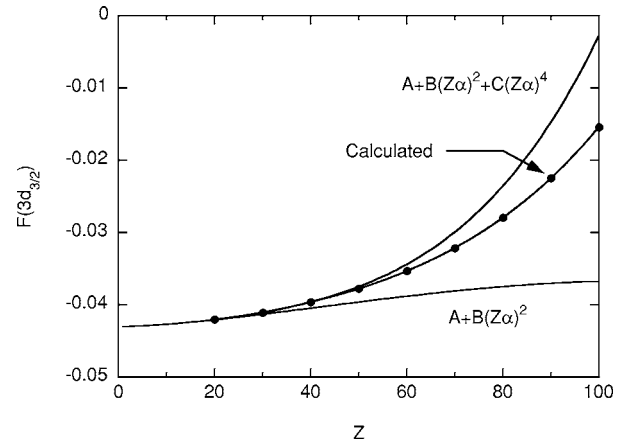

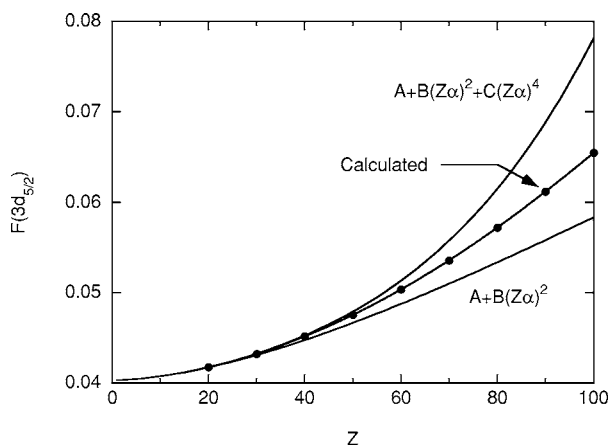FIG. 2. Comparisons between the analytic and calculated hydrogenic results of $F(3d_{3/2})$.

FIG. 3. Comparisons between the analytic and calculated hydrogenic results of $F(3d_{5/2})$.

TABLE II. $F(Z\alpha)$ for the $2s_{1/2}$, $2p_{1/2}$, and $2p_{3/2}$ states of lithiumlike ions with $Z=10-100$.

Z	$2s_{1/2}$	$2p_{1/2}$	$2p_{3/2}$
10	3.4768	−0.0978	0.0365
20	2.9787	−0.0890	0.0903
30	2.5479	−0.0662	0.1221
40	2.2626	−0.0368	0.1484
50	2.0820	−0.0009	0.1730
60	1.9796	0.0427	0.1971
70	1.9423	0.0971	0.2211
80	1.9673	0.1680	0.2451
83	1.9877	0.1938	0.2523
90	2.0607	0.2657	0.2690
92	2.0889	0.2900	0.2738
100	2.2423	0.4110	0.2925

individual states at high l noted above, which lead to much faster partial wave convergence. Fine-structure results shown in Table I are valid to all digits. In particular, at $Z=10$ and 20, the calculated results are the same as those from the following analytic formulas derived from previous equations:

$$F_{fs}(3d) = \frac{1}{12} + 0.022\,058\,416(2)(Z\alpha)^2, \qquad (12)$$

$$F_{fs}(4d) = \frac{1}{12} + 0.025\,825\,877(2)(Z\alpha)^2, \qquad (13)$$

where the lowest order term $1/12$ is entirely due to the one-loop electron anomalous magnetic moment. If we carry out a fit to our data to the form $A+B(Z\alpha)^2+C(Z\alpha)^4$, where A and B are fixed to the values given in the above equations, we find $C=-0.050(2)$ and $-0.067(2)$ for 3d and 4d states, respectively, consistent with but more accurate than those from the difference of fitted coefficients for individual d states shown above. If this is extrapolated to the case of neutral hydrogen, we predict a very small contribution of -0.004 Hz from the higher-order terms in the $Z\alpha$ expansion, showing
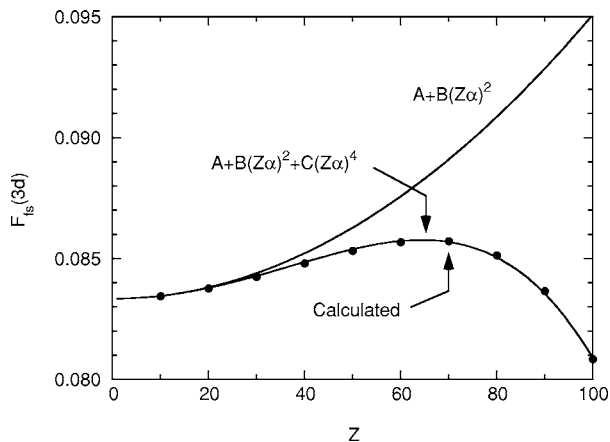
that the expansion to order $(Z\alpha)^2$ is all that is needed for low-Z ions.

Comparisons between our calculated 3d fine-structure results with those from the analytic formulas are shown in Fig. 4. As in individual d-state results shown in Figs. 2 and 3, analytic fine-structure results including up to the $(Z\alpha)^2$ term are seen to be good only up to about $Z=20$. Unlike individual 3d results, however, when the fitted $(Z\alpha)^4$ term is included, analytic fine-structure results are now in excellent agreement with the calculated results for the *entire Z* region. Similar behaviors are found for the 4d fine-structure results and are not shown here. This suggests that higher-order $Z\alpha$-expansion terms, while important for individual d states, largely cancel between fine-structure components.

IV. SCREENED CALCULATIONS

While radiative corrections in few-electron ions can be treated by interpolating or scaling the hydrogenic results, as is done, for example, in Ref. [22], for many-electron systems

FIG. 4. Comparisons between the analytic and calculated hydrogenic fine-structure results of $F(3d)$.

TABLE III. $F(Z\alpha)$ for the $3s_{1/2}$, $3p_{1/2}$, $3p_{3/2}$, $3d_{3/2}$, and $3d_{5/2}$ states of sodiumlike ions with $Z=20-100$.

Z	$3s_{1/2}$	$3p_{1/2}$	$3p_{3/2}$	$3d_{3/2}$	$3d_{5/2}$
20	1.4435	−0.0431	0.0317	−0.0109	−0.0003
30	1.6845	−0.0403	0.0721	−0.0201	0.0061
40	1.6980	−0.0193	0.1070	−0.0242	0.0130
50	1.6742	0.0127	0.1388	−0.0260	0.0190
60	1.6616	0.0549	0.1694	−0.0263	0.0244
70	1.6767	0.1092	0.1997	−0.0255	0.0294
80	1.7296	0.1807	0.2304	−0.0235	0.0342
83	1.7545	0.2067	0.2397	−0.0227	0.0356
90	1.8313	0.2787	0.2616	−0.0203	0.0389
92	1.8588	0.3029	0.2679	−0.0195	0.0399
100	2.0006	0.4222	0.2934	−0.0157	0.0436

TABLE IV. $F(Z\alpha)$ for the $4s_{1/2}$, $4p_{1/2}$, $4p_{3/2}$, $4d_{3/2}$, and $4d_{5/2}$ states of copperlike ions with $Z=40-100$.

Z	$4s_{1/2}$	$4p_{1/2}$	$4p_{3/2}$	$4d_{3/2}$	$4d_{5/2}$
40	0.6045	−0.0070	0.0334	−0.0070	0.0019
50	0.8338	0.0058	0.0649	−0.0117	0.0060
60	0.9758	0.0320	0.0964	−0.0143	0.0109
70	1.0859	0.0711	0.1279	−0.0152	0.0159
80	1.1938	0.1259	0.1597	−0.0146	0.0210
83	1.2288	0.1462	0.1694	−0.0142	0.0226
90	1.3193	0.2030	0.1922	−0.0125	0.0263
92	1.3481	0.2221	0.1988	−0.0119	0.0273
100	1.4829	0.3164	0.2253	−0.0086	0.0315

such as lithiumlike, sodiumlike, and copperlike ions, it is much better to start with a more realistic potential so as to build in the bulk of the screening in lowest order. This approach has been used by Blundell [23] in treating these isoelectronic sequences using a screened core-Hartree potential. Here we use a slightly different model potential, the Kohn-Sham potential [24], defined by

$$V_{KS}(r) = V_C(r) + \alpha \int dr' \frac{1}{r_>} \rho_t(r') - \frac{2}{3} \left[\frac{81}{32\pi^2} r\rho_t(r) \right]^{1/3} \frac{\alpha}{r},$$
(14)

where

$$\rho_t(r) = g_v^2(r) + f_v^2(r) + \sum_a (2j_a + 1)[g_a^2(r) + f_a^2(r)]. \quad (15)$$

Here $V_C(r)$ is the nuclear Coulomb field, including finite nuclear size using a Fermi distribution, and $g(r)$ and $f(r)$ are the upper and lower radial components of Dirac wave functions, determined self-consistently. For lithiumlike ions, $v=2s$ and the sum is over a heliumlike core. For sodiumlike ions, $v=3s$ and the sum is over a neonlike core. Finally for
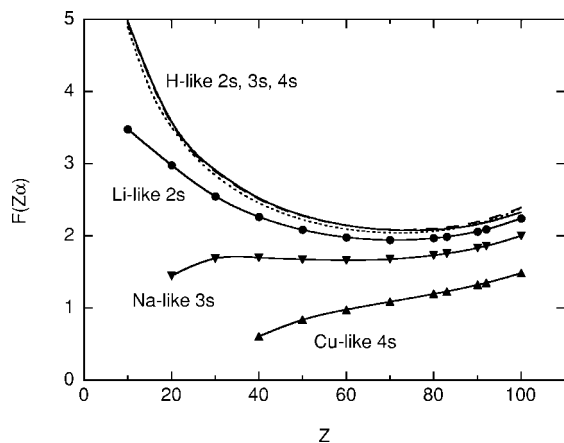

FIG. 5. Comparisons between the hydrogenic and screened self-energy functions $F(Z\alpha)$ for the ns states. Dotted, dashed, and solid lines without symbols are hydrogenic $2s$, $3s$, and $4s$ results, respectively. Solid lines with symbols are Kohn-Sham results.
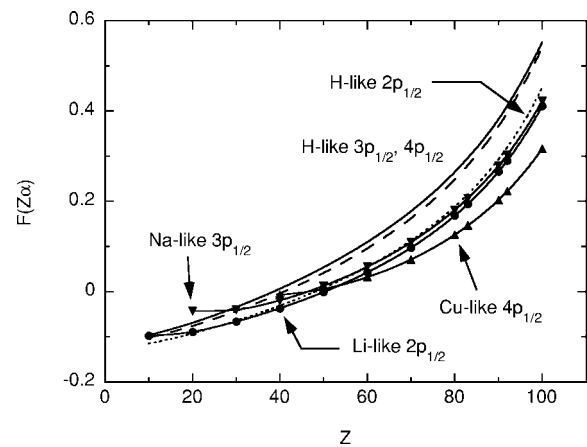

FIG. 6. Comparisons between the hydrogenic and screened self-energy functions $F(Z\alpha)$ for the $np_{1/2}$ states. Dotted, dashed, and solid lines without symbols are hydrogenic $2p_{1/2}$, $3p_{1/2}$, and $4p_{1/2}$ results, respectively. Solid lines with circles, inverted triangles, and triangles are Li-like $2p_{1/2}$, Na-like $3p_{1/2}$, and Cu-like $4p_{1/2}$ Kohn-Sham results, respectively.

copperlike ions, $v=4s$ and the sum is over a nickel-like core. These potentials give results similar to the Hartree-Fock potential, which we do not use because its nonlocality makes it difficult to incorporate into a complete QED framework such as the S-matrix theory. The factor $2/3$ in the Kohn-Sham potential can take other values: for example, 1 for the Slater potential and 0 for the Hartree potential. However, we have invariably found good agreement with experiment when using the Kohn-Sham potential and would recommend that it be generally adopted as a standard for the many-electron problem. While a great advantage of restricting oneself to the hydrogenic self-energy is that it is a natural standard, it can only be applied to ions with many electrons through interpolating or scaling procedures or perturbation theory, which become more and more problematic as the number of electrons in the ion increases.

We present, in Tables II–IV, results for $n=2$ lithiumlike ions, $n=3$ sodiumlike ions, and $n=4$ copperlike ions, respectively. While our interest is in d states, results for the s and p
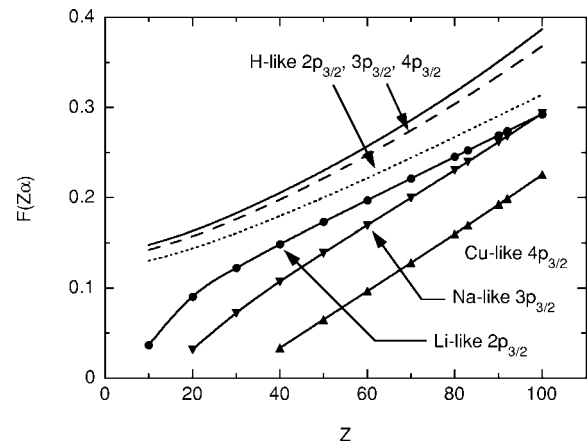

FIG. 7. Comparisons between the hydrogenic and screened Kohn-Sham self-energy functions $F(Z\alpha)$ for the $np_{3/2}$ states.

FIG. 8. Comparisons between the hydrogenic and screened Kohn-Sham self-energy functions $F(Z\alpha)$ for the $nd_{3/2}$ states.
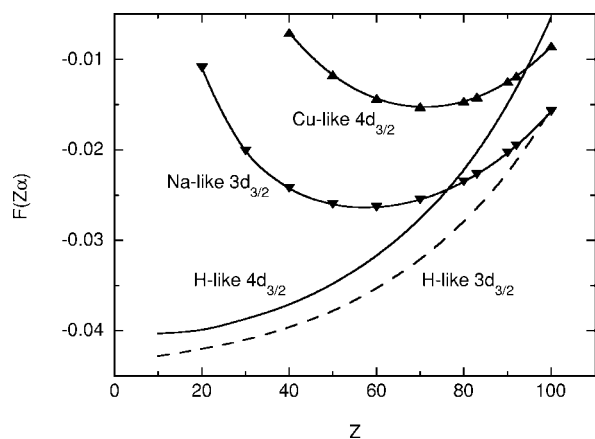

FIG. 9. Comparisons between the hydrogenic and screened Kohn-Sham self-energy functions $F(Z\alpha)$ for the $nd_{5/2}$ states.

states are also shown for completeness. In Fig. 5, our screened ns self-energies are compared with the hydrogenic results of Mohr and co-workers [5,6]. It can be seen that hydrogenic results of $F(Z\alpha)$ for $2s$, $3s$, and $4s$ are very similar throughout the Z range, but such is not the case when screening corrections are included. In fact, with more and more electrons in the ion, the screened $F(Z\alpha)$ functions for the ns states deviate more and more from the hydrogenic results. Similar comparisons are made for the $np_{1/2}$, $np_{3/2}$, $nd_{3/2}$, and $nd_{5/2}$ results in Figs. 6–9, respectively. Except for $np_{1/2}$, all screened self-energies are found to be quite different from the corresponding hydrogenic results.

V. DISCUSSION

While little data involving the nd states in high-Z sodium-like and copperlike systems are available, a high-precision experiment on transition energies involving the 4d state for copperlike ions has recently been carried out [14], and we discuss these measurements in some detail so as to show the role of radiative corrections in screened potentials for this case. The transition is $3d^{10}4p$ $(J=1/2)-3d^{10}4d$ $(J=3/2)$, and the energies for Bi^{54+}, Th^{61+}, and U^{63+} have been determined to be 366.72(2), 491.94(10), and 535.15(5) eV, respectively. It is quite straightforward to carry out relativistic many-body perturbation theory (MBPT) calculations [25] for these transitions using, for consistency, a Kohn-Sham potential. The results of a calculation including Coulomb interactions through third order, instantaneous Breit and Breit-Coulomb interactions, and the effect of retardation on the Breit interaction are 367.21, 492.42, and 535.69 eV. The difference between experiment and this "structure" calculation implies QED effects of -0.24, -0.48, and -0.54 eV. With vacuum polarizations estimated to be 0.09, 0.19, and 0.24 eV from expectation values of the Uehling potential calculated with Kohn-Sham wave functions, the deduced self-energy corrections are given by -0.33, -0.67, and -0.78 eV. Possible errors from the combined theoretical and experimental uncertainties are likely to be around 10–20 %. Were one to
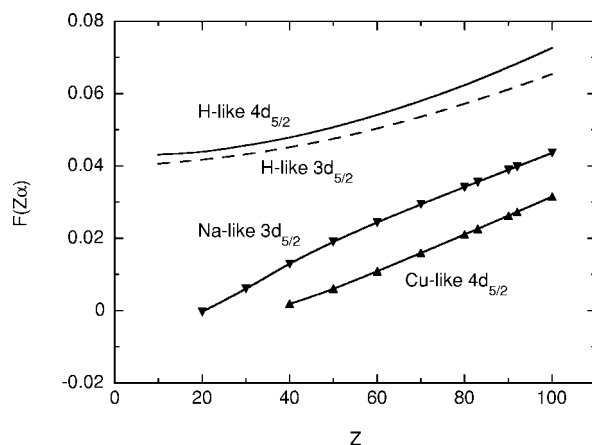
use hydrogenic values for the Lamb shift, one would get -0.79, -1.37, and -1.59 eV, which are twice as big as the deduced values, indicating the presence of a significant level of screening. Likewise, interpolating the hydrogenic values to $Z_{\text{eff}}=Z-28=55$, 62, and 64 for copperlike Bi^{54+}, Th^{61+}, and U^{63+}, respectively, leads to overcorrected results of -0.06, -0.12, and -0.14 eV which are too small by a factor of 5. If we instead use the Kohn-Sham values from Table III, we get the much more reasonable set of values -0.40, -0.74, and -0.88 eV. Thus this relatively simple procedure gives self-energy results which are consistent with experiment to within 20% and are almost within the expected error bars of the deduced self-energies.

To explain the remaining difference involves a number of rather complex issues which we have discussed before elsewhere [26]. They involve the direct evaluation of screening corrections to the one-loop self-energy and vacuum polarization diagrams (also discussed by Indelicato and Mohr in Ref. [27]), the inclusion of recoil corrections, and the correct treatment of "two-photon" Feynman diagrams beyond the dominant two-photon exchange graphs which have been included in MBPT. The Wichmann-Kroll corrections to the vacuum polarization, though expected to be small, have to be evaluated also. In the case of $2s$-$2p$ transitions in lithiumlike Bi^{80+}, we have shown that the Kohn-Sham potential is a much better starting point than the Coulomb potential for treating these small corrections [26]. We expect the same to be true here, especially since there are significantly more electrons in copperlike than in lithiumlike ions. We are presently extending the S-matrix methods developed for lithium-like bismuth to the sodiumlike case, and the same methods should also be applicable to copperlike ions.

[1] P. J. Mohr, in *Atomic, Molecular and Optical Physics Handbook*, edited by G. W. F. Drake (AIP, Woodbury, NY, 1996).

[2] G. E. Brown, J. S. Langer, and G. W. Schaefer, Proc. R. Soc. London, Ser. A **251**, 92 (1959).

[3] A. M. Desiderio and W. R. Johnson, Phys. Rev. A **3**, 1267 (1971).

[4] P. J. Mohr, Ann. Phys. (N.Y.) **88**, 26 (1974).

[5] P. J. Mohr and Y.-K. Kim, Phys. Rev. A **45**, 2727 (1992).

[6] P. J. Mohr, Phys. Rev. A **46**, 4421 (1992).

[7] P. J. Mohr and G. Soff, Phys. Rev. Lett. **70**, 158 (1993).

[8] N. J. Snyderman, Ann. Phys. (N.Y.) **211**, 43 (1991).

[9] K. T. Cheng, W. R. Johnson, and J. Sapirstein, Phys. Rev. A **47**, 1817 (1993).

[10] S. A. Blundell and N. J. Snyderman, Phys. Rev. A **44**, R1427 (1991).

[11] H. Persson, I. Lindgren, and S. Salomonson, Phys. Scr. **T46**, 125 (1993).

[12] V. A. Yerokhin and V. M. Shabaev, Phys. Rev. A **60**, 800 (1999).

[13] L. Labzowsky, I. Goidenko, M. Tokman, and P. Pyykkö, Phys. Rev. A **59**, 2707 (1999).

[14] E. Trabert, P. Beiersdorfer, K. B. Fournier, and M. H. Chen, Can. J. Phys. **82**, 1 (2004).

[15] G. E. Brown and G. W. Schaefer, Proc. R. Soc. London, Ser. A **233**, 527 (1956).

[16] S. A. Blundell, Phys. Rev. A **46**, 3762 (1992).

[17] T. Hahn, Comput. Phys. Commun. **168**, 78 (2005).

[18] J. Sapirstein and K. T. Cheng, Phys. Rev. A **68**, 042111 (2003).

[19] Eric-Olivier Le Bigot, Paul Indelicato, and Peter J. Mohr, Phys. Rev. A **64**, 052508 (2001).

[20] Eric-Olivier Le Bigot, Ulrich D. Jentschura, Peter J. Mohr, Paul Indelicato, and Gerhard Soff, Phys. Rev. A **68**, 042101 (2003).

[21] S. P. Goldman and G. W. F. Drake, Phys. Rev. A **61**, 052513 (2000).

[22] Y.-K. Kim, D. H. Baik, P. Indelicato, and J. P. Desclaux, Phys. Rev. A **44**, 148 (1991).

[23] S. A. Blundell, Phys. Rev. A **47**, 1790 (1993).

[24] R. Cowan, *The Theory of Atomic Structure and Spectra* (University of California Press, Berkeley, 1981), Chap. 7, Sec. 7-11.

[25] W. R. Johnson, S. A. Blundell, and J. Sapirstein, Phys. Rev. A **42**, 1087 (1990).

[26] J. Sapirstein and K. T. Cheng, Phys. Rev. A **64**, 022502 (2001).

[27] P. Indelicato and P. J. Mohr, Phys. Rev. A **63**, 052507 (2001).